length and 4 µm drain-to-source spacing is shown in Fig. 3. This results in a breakdown voltage of ~-10 V for 1 mA/mm gate current density, which is very suitable for power applications. Fig. 4 shows a typical I-V curve for 0.5 µm gate length and a 2.5 µm source drain spacing device. The gate bias ranges from -8 to 1 V. The device demonstrates good pinch-off voltage characteristics. This allows good isolating buffer growth on silicon substrate. Moreover, the drain current density is > 100 mA/mm at V_{gs} = 1 V and V_{ds} = 30 V. This high drain-to-source voltage is also very appropriate for power applications. Finally, an extrinsic transconductance G_m > 30 mS/mm at V_{ds} = 20 V can be observed in Fig. 5, which confirms the good pinch-off characteristic.

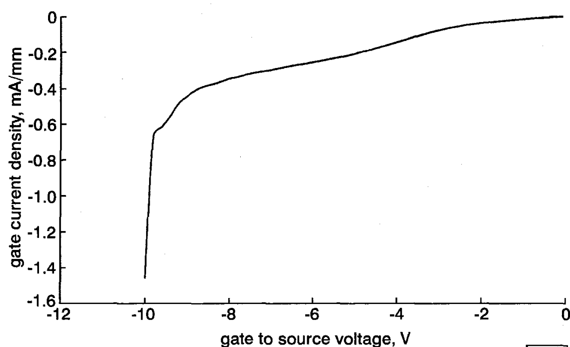

Fig. 3 *Gate current density of 100 * 2 µm² device*

V_{gs} = 0 to -10 V

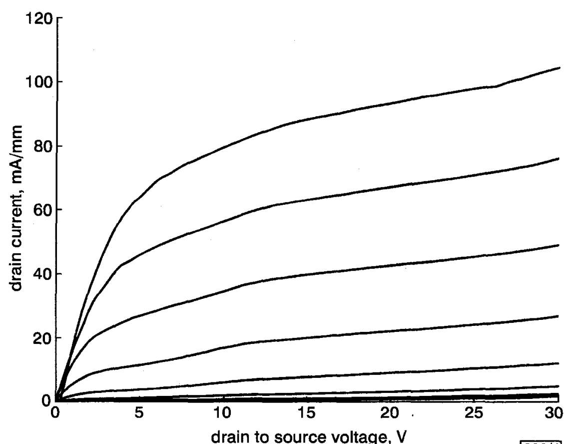

Fig. 4 *I-V characteristics of 100 * 0.5 µm² device*

V_{gs} = -8 to 0 V (step 1 V)

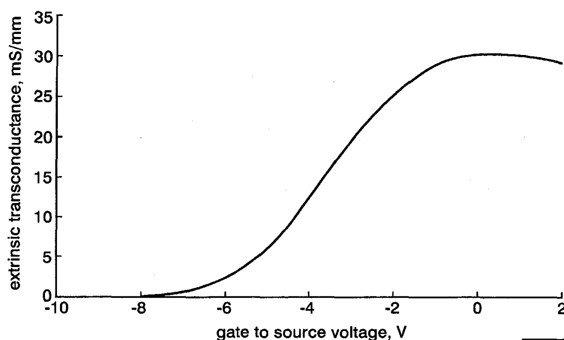

Fig. 5 *Extrinsic transconductance for 100 * 0.5 µm² device*

V_{gs} = -8 to 2 V and V_{ds} = 20 V

Conclusion: The first GaN MESFETs on (111) Si substrates have been realised using low-pressure metal-organic vapour phase epitaxy. The devices demonstrate good pinch-off voltage characteristics and high breakdown voltage in diode and transistor configuration. This good holding voltage and the possibility of realising an isolating buffer on silicon substrate mean that GaN MESFETs on Si (111) are of particular interest in respect of future power devices and wireless communication applications.

© IEE 2001
28 May 2001
Electronics Letters Online No: 20010740
DOI: 10.1049/el:20010740

V. Hoël, Y. Guhel, B. Boudart, C. Gaquière and J.C. De Jaeger (*IEMN, UMR-CNRS 8520, USTL, Avenue Poincaré – B.P. 69, 59652 Villeneuve d'Ascq Cedex, France*)

E-mail: Hoel@iemn.univ-lille1.fr

H. Lahrèche and P. Gibart (*CRHEA-CNRS, Rue B. Gregory, Sophia Antipolis, 06560 Valbonne, France*)

References

1 *Compound Semicond.*, 2000, **6**, (1), p. 13

2 WU, Y.F., KELLER, B.P., FINI, J., PUSL, J., LE, M., NGUYEN, N.X., NGUYEN, C., WIDMAN, D., KELLER, S., DENBAARS, S.P., and MISHRA, U.K.: 'Short-channel $Al_{0.5}Ga_{0.5}N$/GaN MODFETs with power density > 3 W/mm at 18 GHz', *Electron. Lett.*, 1997, **33**, (20), pp. 1742–1743

3 GAQUIÈRE, C., TRASSAERT, S., BOUDART, B., and CROSNIER, Y.: 'High-power GaN MESFET on sapphire substrate', *IEEE Microw. Guid. Wave Lett.*, 2000, **10**, (1) pp. 19–20

4 CHUMBES, E.M., SCHREMER, A.T., SMART, J.A., HOGUE, D., KOMIAK, J., and SHEALY, J.R.: 'Microwave performance of AlGaN/GaN high electron mobility transistors on Si(111) substrates'. IEEE Int. Electron Devices Mtg., 1999, pp. 397–400

5 LAHRÈCHE, H., BOUSQUET, V., LAÜGT, M., TOTTEREAU, O., VENNEGUES, P., BEAUMONT, B., and GIBART, P.: 'High quality GaN on Si(111) using $(AlN/GaN)_x$ superlattice and maskless ELO'. Int. Conf. Silicon Carbide and Related Materials, 1999, pp. 1487–1490

6 LAHRÈCHE, H., VENNEGUES, P., TOTTEREAU, O., LAÜGT, M., LORENZINI, P., LEROUX, M., BEAUMONT, B., and GIBART, P.: 'Optimisation of AlN and GaN growth by metalorganic vapor-phase epitaxy (MOVPE) on Si(111)', *J. Cryst. Growth*, 2000, **217**, pp. 13–35

Transferred-substrate InP/InGaAs/InP double heterojunction bipolar transistors with f_{max} = 425 GHz

S. Lee, H.J. Kim, M. Urteaga, S. Krishnan, Y. Wei, M. Dahlström and M. Rodwell

InP/InGaAs/InP double heterojunction bipolar transistors (DHBTs) with f_{max} = 425 GHz and f_τ = 141 GHz using transferred-substrate technology are reported. This is the highest reported f_{max} for a DHBT. The breakdown voltage BV_{CEO} is 8 V at $J_C = 5 \times 10^4$ A/cm² and the DC current gain β is 43.

Introduction: Very wide bandwidth double heterojunction bipolar transistors (DHBTs) enables high-power amplifiers at 94 and 180 GHz, microwave analogue digital converters, microwave direct digital frequency synthesis, fibre optic transmission at > 40 Gbit/s and wireless data networks at frequencies above 100 GHz [1]. Transferred substrate single heterojunction bipolar transistors (SHBTs) have demonstrated very high bandwidth and are potential candidates for very high-speed integrated circuit applications [2, 3]. The transferred substrate SHBTs, however, have very low breakdown voltage, $BV_{CEO} \simeq 1.5$ V. In this Letter we report an InP/InGaAs/InP transferred substrate DHBT with record f_{max} and a high breakdown voltage, BV_{CEO} = 8 V at $J_C \simeq 5 \times 10^4$ A/cm². Extrapolating at 20 dB/decade, the power gain cutoff frequency f_{max} = 425 GHz and the current gain cutoff frequency f_τ = 141 GHz. The record f_{max} is due to the scaling of HBT junction widths and the elimination of collector series resistance through the use of a Schottky collector contact.

Experiment: Table 1 shows the MBE-grown layer structure. As heat was removed through the emitter, a thin 300 Å InGaAs emitter contact layer was used to improve thermal conductivity. We used compositionally-graded InGaAs/InAlAs layers at each interface between the InGaAs base and the InP emitter and collector.

The base layer is 400 Å thick and is Be-doped at $4 \times 10^{19}/cm^3$. To reduce the base transit time, we designed the base layer with 52 meV bandgap grading, introduced by varying the Ga:In ratio.

Table 1: Layer structure of MBE-grown InP/InGaAs/InP DHBT

Layer	Material	Doping	Thickness
			Å
Emitter cap	InGaAs	1×10^{19} : Si	300
Grade	InGaAs/InAlAs	1×10^{19} : Si	200
N^{++} emitter	InP	1×10^{19} : Si	900
N emitter	InP	8×10^{17} : Si	300
Grade	InGaAs/InAlAs	8×10^{17} : Si	233
Grade	InGaAs/InAlAs	8×10^{17} : Be	67
Base	InGaAs	4×10^{19} : Be	400
Grade	InGaAs/InAlAs	1×10^{16} : Si	480
Delta doping	InP	1.6×10^{18} : Si	20
Collector	InP	1×10^{16} : Si	2500

The $0.5 \times 8\,\mu m^2$ emitter contact metal was defined by optical projection lithography. The emitter-base mesa was formed by selective wet etching and nonselective citric-based wet etching. Selective wet etching was used for base mesa isolation. Subsequent steps were similar to the transferred substrate HBT process [3]. The $1.2 \times 8.75\,\mu m^2$ Schottky collector contact was made on a 3000 Å thick InP collector layer after removing the S.I. InP substrate.

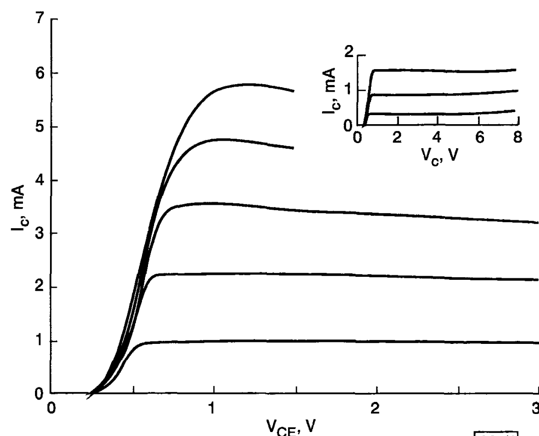

Fig. 1 *Common emitter DC characteristics of 0.5 × 8 µm² emitter device*

I_b step = 30 µA
BV_{CEO} = 8 V at $J_C \simeq 5 \times 10^4$ A/cm²

Fig. 1 shows the common emitter DC characteristic. The BV_{CEO} = 8 V at $J_C \simeq 5 \times 10^4$ A/cm² and the DC current gain β = 43. The devices were characterised by on-wafer network analysis from 1 to 45 GHz and 75 to 110 GHz. With high f_{max} HBTs, C_{cb} is low, resulting in a low reverse transmission S_{12}. Small measurement errors in S_{12} arising from parasitic probe-probe electromagnetic coupling then result in significant measurement errors in determination of the transistor C_{cb} and f_{max}. To obtain accurate measurements, the network analyser was calibrated with on-wafer line-reflect-line (LRL) microstrip calibration standards. Reference planes are offset from the probe pads by 230 µm, resulting in a minimum 460 µm probe-probe separation, and reduced probe-probe coupling.

The cutoff frequencies f_τ = 139 GHz and f_{max} = 425 GHz were measured at I_C = 4.5 mA and V_{CE} = 1.9 V, as determined by a least-squares fit to the data (Fig. 2). Fig. 3 shows the collector current dependence on cutoff frequencies. The highest f_τ = 141 GHz was measured at I_C = 5.2 mA and V_{CE} = 1.9 V. Due to the offset on-wafer LRL calibration, the 45 MHz to 45 GHz data is well-matched to the 75 to 110 GHz data and gain slopes are close to the expected −20 dB/decade.

To further improve f_{max}, a carbon doped base at > $10^{20}/cm^3$ can be employed, improving both the base sheet and contact resistance. We ascribe the relatively low measured f_τ to current blocking at the base-collector interface, and are presently investigating improved heterojunction grading of the base-collector junction.

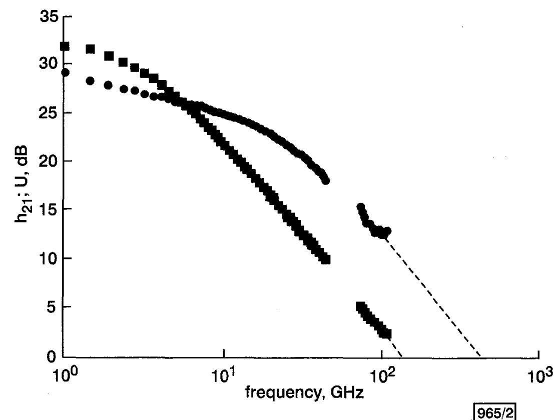

Fig. 2 *Small signal current and power gains against frequency characteristics at I_C = 4.5 mA and V_{CE} = 1.9 V*

● *U*
■ h_{21}

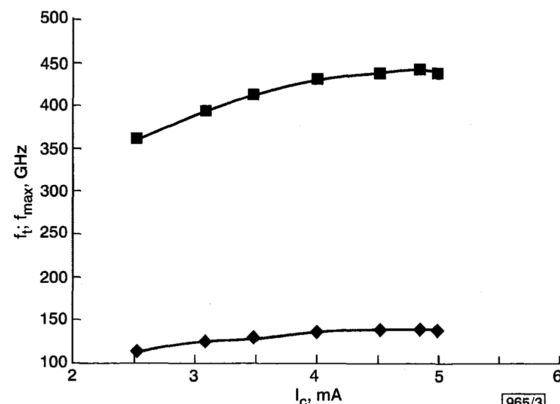

Fig. 3 *Variation of f_τ and f_{max} with collector current at V_{CE} = 1.9 V*

—◆— f_τ
—■— f_{max}

Conclusion: We have fabricated InP/InGaAs/InP DHBTs using substrate transfer. The emitter and base mesa structure were formed by wet etching techniques. The highest f_{max} = 425 GHz was measured in a device with $0.5 \times 8\,\mu m^2$ emitter contact area. These results demonstrate the promise of InP/InGaAs/InP transferred substrate DHBTs for high speed and high power applications.

Acknowledgment: This work was supported by the ONR under grant number N00014-01-1-0065.

© IEE 2001

4 June 2001
Electronics Letters Online No: 20010728
DOI: 10.1049/el:20010728

S. Lee, H.J. Kim, M. Urteaga, S. Krishnan, Y. Wei, M. Dahlström and M. Rodwell (*Department of Electrical and Computer Engineering, University of California, Santa Barbara, CA 93106, USA*)

E-mail: sangmin@ece.ucsb.edu

References

1 RODWELL, M., LEE, Q., MENSA, D., GUTHRIE, J., JAGANATHAN, S., MATHEW, T., and LONG, S.: '48 GHz digital ICs using transferred substrate HBT'. IEEE GaAs IC Symp. Tech. Dig., 1998, pp. 113–117

2 LEE, Q., AGARWAL, B., PULLELA, R., MENSA, D., GUTHRIE, J., SAMOSKA, L., and RODWELL, M.: 'A >400 GHz f_{max} transferred-substrate heterojunction bipolar transistor IC technology', *IEEE Electron Device Lett.*, 1998, **19**, pp. 77–79

3 LEE, Q., MARTIN, S.C., MENSA, D., SMITH, R.P., GUTHRIE, J., and RODWELL, M.J.W.: 'Submicron transferred-substrate heterojunction bipolar transistors', *IEEE Electron Device Lett.*, 1999, **20**, (8), pp. 396–398

Analytical design of higher-order differentiators using least-squares technique

G. Mollova and R. Unbehauen

New, simple analytic closed-form relations for least-squares design of higher-order differentiators are presented. Using this approach, solving a system of linear equations for fullband differentiators is avoided. Numerical and graphical results are given.

Introduction: Different methods have been proposed recently for designing higher-order differentiators [1 – 4], e.g. the minimax approach, the eigenfilter method, the least-squares technique. An analytical least-squares solution for first-order differentiators has been shown [5]. In this Letter we present new closed-form expressions for least-squares design of arbitrary higher-order digital differentiators. Fullband and non-fullband cases are considered.

	odd k (N even)	even k (N even)
$d(n)$	$2^{-k}\sum_{l=1}^{(k+1)/2}\frac{(-1)^{l+n}\pi^{1-2l}r_1}{(n-1/2)^{2l}}, 1\leq n\leq N/2$	$2^{-k}\sum_{l=1}^{k/2}\frac{(-1)^{l+n+1}h}{\pi^{2l-1}n^{2l}}, 1\leq n\leq (N-1)/2$ $\frac{\pi}{2^k(k+1)}, n=0$
$q(n,m)$	$0, n\neq m$ $\pi/2, n=m, 1\leq n,m\leq N/2$	$0, n\neq m$ $\pi/2, n=m\neq 0$ $\pi, n=m=0, 0<n,m<(N-1)/2$
$b(n)$	$2^{1-k}\sum_{l=1}^{(k+1)/2}\frac{(-1)^{l+n}r_1}{\pi^{2l}(n-1/2)^{2l}}, 1\leq n\leq N/2$	$2^{1-k}\sum_{l=1}^{k/2}\frac{(-1)^{l+n+1}h}{(\pi.n)^{2l}}, 1\leq n\leq (N-1)/2$ $\frac{1}{2^k(k+1)}, n=0$

125/1

Fig. 1 *Fullband higher-order differentiators* ($\omega_p = \pi$)

Higher-order differentiators: An ideal kth-order digital differentiator (DD) has a frequency response $H_i(e^{j\omega}) = D(\omega)e^{jk\pi/2}$, where $D(\omega) = (\omega/2\pi)^k$ for $0 \leq \omega \leq \omega_p \leq \pi$. Here ω_p denotes the passband edge frequency. A nonrecursive filter with an antisymmetrical impulse response of length N [3, 4] can be used for the design of odd-order differentiators with a frequency response:

$$H(e^{j\omega}) = M(\omega)e^{j(\pi/2-\omega(N-1)/2)}$$

where the real-valued $M(\omega)$ is

$$M(\omega) = \begin{cases} \sum_{n=1}^{(N-1)/2} b(n)\sin n\omega & N \text{ odd} \\ \sum_{n=1}^{N/2} b(n)\sin(n-1/2)\omega & N \text{ even} \end{cases} \qquad (1)$$

For the design of an even-order DD a linear-phase filter with symmetric impulse response could be applied. In this case $H(e^{j\omega}) = M(\omega)e^{-j\omega(N-1)/2}$, where

$$M(\omega) = \begin{cases} \sum_{n=0}^{(N-1)/2} b(n)\cos n\omega & N \text{ odd} \\ \sum_{n=1}^{N/2} b(n)\cos(n-1/2)\omega & N \text{ even} \end{cases} \qquad (2)$$

By minimising the mean-square error function $Emse = (1/\pi)\int_0^{\omega_p}[D(\omega) - M(\omega)]^2 d\omega$, a required higher-order DD can be designed. As a result we obtain a system of linear equations $\mathbf{Qb} = \mathbf{d}$, where [3]: $\mathbf{Q} = \int_0^{\omega_p}\mathbf{c}(\omega)\mathbf{c}^T(\omega)d\omega$, $\mathbf{d} = \int_0^{\omega_p}D(\omega)\mathbf{c}(\omega)d\omega$, and $M(\omega) = \mathbf{b}^T\mathbf{c}(\omega)$. For the case of odd k

$$\mathbf{c}(\omega) = \begin{cases} \left[\sin\omega, \sin 2\omega, ..., \sin\left(\frac{N-1}{2}\omega\right)\right]^T & N \text{ odd} \\ \left[\sin\frac{1}{2}\omega, \sin\frac{3}{2}\omega, ..., \sin\left(\frac{N-1}{2}\omega\right)\right]^T & N \text{ even} \end{cases} \qquad (3)$$

$$\mathbf{b} = \begin{cases} [b(1), b(2), ..., b((N-1)/2)]^T & N \text{ odd} \\ [b(1), b(2), ..., b(N/2)]^T & N \text{ even} \end{cases} \qquad (4)$$

and for even k

$$\mathbf{c}(\omega) = \begin{cases} \left[1, \cos\omega, ..., \cos\left(\frac{N-1}{2}\omega\right)\right]^T & N \text{ odd} \\ \left[\cos\frac{1}{2}\omega, \cos\frac{3}{2}\omega, ..., \cos\left(\frac{N-1}{2}\omega\right)\right]^T & N \text{ even} \end{cases} \qquad (5)$$

$$\mathbf{b} = \begin{cases} [b(0), b(1), ..., b((N-1)/2)]^T & N \text{ odd} \\ [b(1), b(2), ..., b(N/2)]^T & N \text{ even} \end{cases} \qquad (6)$$

where the superscript T denotes the vector transpose operation.

Analytical expressions: The elements of $\mathbf{Q}$ and $\mathbf{d}$ are usually evaluated by numerical integration. Here we show that a closed-form solution is also possible.

Relations for the entries of $\mathbf{Q}$ in the case of odd-order k are identical to those for the first-order DD [5]. Applying the formula given in [2], we obtain for the elements of $\mathbf{d}$

$$d(n) = \begin{cases} \frac{1}{(2\pi)^k}\sum_{l=1}^{(k+1)/2}\left[(-1)^l\frac{r\omega_p^{k-2l+2}\cos n\omega_p}{n^{2l-1}} + (-1)^{l+1}\frac{r_1\omega_p^{k-2l+1}\sin n\omega_p}{n^{2l}}\right] \\ \qquad N \text{ odd}, 1 \leq n \leq (N-1)/2 \\ \frac{1}{(2\pi)^k}\sum_{l=1}^{(k+1)/2}\left[(-1)^l\frac{r\omega_p^{k-2l+2}\cos(n-1/2)\omega_p}{(n-1/2)^{2l-1}} + (-1)^{l+1}\frac{r_1\omega_p^{k-2l+1}\sin(n-1/2)\omega_p}{(n-1/2)^{2l}}\right] \\ \qquad N \text{ even}, 1 \leq n \leq N/2 \end{cases} \qquad (7)$$

where

$$r = k(k-1)\cdots(k-2l+3) \qquad 2 \leq l \leq (k+1)/2$$
$$r_1 = k(k-1)\cdots(k-2l+2) \qquad 1 \leq l \leq (k+1)/2$$
and $r = 1$ for $l = 1$

For fullband odd-order DD ($\omega_p = \pi$, N even) we get simpler relations for the elements of $\mathbf{d}$ and $\mathbf{Q}$ which are shown in Fig. 1. By this means solving the system of linear equations given in the previous Section is avoided. An exact formula for the vector $\mathbf{b}$ is obtained (Fig. 1) and $M(\omega)$ can be directly calculated using eqn. 1.

The elements of the matrix $\mathbf{Q}$ for even-order DD are derived as

$$q(n,m) = \begin{cases} \frac{\omega_p}{2}[\text{sinc}(n+m-f)\omega_p + \text{sinc}(n-m)\omega_p] & n \neq m \\ \frac{\omega_p}{2}[1 + \text{sinc}(2n-f)\omega_p] & n = m \neq 0 \\ \omega_p & n = m = 0 \\ \text{and } f = 0 \text{ for } 0 \leq n,m \leq \frac{N-1}{2} & N \text{ odd} \\ \qquad f = 1 \text{ for } 1 \leq n,m \leq N/2 & N \text{ even} \end{cases} \qquad (8)$$

where $\text{sinc}x = \sin x/x$. Using the formula from [2] we obtain

$$d(n) = \begin{cases} \frac{\omega_p^{k+1}\text{sinc}\, n\omega_p}{(2\pi)^k} + \frac{1}{(2\pi)^k}\sum_{l=1}^{k/2}\left[(-1)^{l+1}\frac{h\omega_p^{k-2l+1}\cos n\omega_p}{n^{2l}} + (-1)^{l+2}\frac{h_1\omega_p^{k-2l}\sin n\omega_p}{n^{2l+1}}\right] \\ \qquad N \text{ odd}, 1 \leq n \leq (N-1)/2 \\ \frac{\omega_p^{k+1}}{(2\pi)^k(k+1)} \qquad N \text{ odd}, n = 0 \\ \frac{\omega_p^{k+1}\text{sinc}(n-1/2)\omega_p}{(2\pi)^k} + \frac{1}{(2\pi)^k}\sum_{l=1}^{k/2}\left[(-1)^{l+1}\frac{h\omega_p^{k-2l+1}\cos(n-1/2)\omega_p}{(n-1/2)^{2l}} + (-1)^{l+2}\frac{h_1\omega_p^{k-2l}\sin(n-1/2)\omega_p}{(n-1/2)^{2l+1}}\right] \\ \qquad N \text{ even}, 1 \leq n \leq N/2 \end{cases} \qquad (9)$$